

ORIGINAL RESEARCH PAPER

Experimental Investigation of Impact Damage Response of Sandwich Panels with Epoxy/woven-Fiberglass/nano-Silica Composite Face-sheets

M. Mahdipour Jalilian^a, S. Feli^{*,b}

^aMechanical Engineering Department, Kermanshah Branch, Islamic Azad University, Kermanshah, Iran.

^bMechanical Engineering Department, Razi University, Kermanshah, Iran.

Article info

Article history:

Received 05 February 2020

Received in revised form

10 May 2020

Accepted 24 May 2020

Keywords:

Sandwich panel

Nano-silica

Low velocity impact

Interlaminar shear strength

Delamination threshold force

Abstract

In this paper by using the three-point bending and low velocity impact tests, the impact damage response of Polyurethane cored sandwich panels with hybrid nanocomposites face-sheets is investigated. The face-sheets are made of epoxy/woven-fiberglass/nano-silica composite. Three-point bending test is used for determination of static threshold delamination force, and static and dynamic Interlaminar shear strength has been calculated. Furthermore, low velocity impact tests are performed on a sandwich panel and contact forces history, lateral deflection of the contact point and the absorbed energy of top face-sheets are obtained. The dynamic threshold delamination force has been used to predict the delamination damage mode in low velocity impact tests on sandwich panel. Finally, the delamination damage area is investigated theoretically and experimentally and the correction factor is associated with allowable shear stress is determined. Moreover, the effect of nano-silica particles on delaminations threshold forces, Interlaminar shear strengths, contact force, contact duration, deflection of contact point, energy absorption of top face-sheet and damage area caused by delamination is studied.

1. Introduction

A structure with a relative soft core placed between two stiffer face-sheets is called a sandwich panel. Due to high strength to weight, the sandwich panels are used in airplanes, spacecraft and so on. Face-sheets may be metal, composites or etc. Composites in general are made of two major parts: matrix and reinforcement(s). The reinforcement part of composites can be particles, fibers and laminar-reinforcements. By reduction of the reinforcement part dimensions from micro to nano meters, the nanocomposite is obtained. Often by nano-scaling, the mechanical properties improve. On the

other hand, the core of sandwich panel is commonly honeycomb, Z-pinned or foam. In the following, two common experiments for determination of the damage response of composites or sandwich panels with composite face-sheets are investigated: Three-point Bending (TPB) and Low Velocity Impact (LVI). TPB is one of the tests, which can obtain the flexural properties of a (nano-) composite. For example Azzam and Li [1] investigated the response of composites to TPB test and found that the arrangement of layers affect the occurrence of damage modes. Farrokhhabadi et al. studied the mechanical behavior of multilayer corru-

*Corresponding author: S. Feli (Associate Professor)

E-mail address: felisaeid@gmail.com

<http://dx.doi.org/10.22084/jrstan.2020.20984.1129>

ISSN: 2588-2597

gated core laminated composite sandwich panel subjected to quasi-static three-point bending experimentally and numerically [2]. The numerical results showed good agreement with experimental ones. Pyrzowski and Sobczyk investigated the behavior of laminated sandwich beams (FRP face sheet - PET foam core - FRP face sheet) numerically and compared the numerical simulation with experiments [3]. In another study, Lim and Lee [4] investigated the failure modes of PVC cored sandwich with Epoxy/E-glass face-sheet beams under static TPB test and impact loadings experimentally and using finite elements method and showed that the FEM has good accuracy in prediction of damages. Some researchers investigated the failure or damage modes caused by LVI tests. Yang and Cantwell [5] investigated the damage results from impact loading and found that required impact force to initiate the delamination is localized (independent of planar geometry) and varies linearly with $t^{3/2}$, where t is thickness of plate. This independency is also reported in other works [6, 7]. It has also been reported that damage initiation is independent of boundary conditions while depends on the radius of impactor. Some researchers tried to show the similarity between failure modes of low velocity impact and quasi-static loadings [8, 9]. Swanson [10] indicated that the impact loading on a plate can be approximated as a quasi-static loading if the ratio of impactor mass to lumped mass of panel is greater than ten. When the interlaminar shear stresses exceed than a critical value called interlaminar shear strength (ILSS), delamination mode of damage occurs. Ray [11] investigated the ILSS of a fiberglass/epoxy composite plate with various crosshead speeds in TPB tests and found that by increasing the crosshead speed the ILSS increases. Similar study was done by Hallet et al. [12] on carbon fiber/epoxy and it was observed that at high strain rates, ILSS was 24% higher than quasi-static loading. In another study the ILSS showed about 25% increment in impact loading than quasi-static ones [5]. Sutherland and Soares [13] showed that threshold delamination force depends on $ILSS^{3/2}$. Another study by Schubel et al. [14] verifies the increment of delamination threshold force in dynamic tests in comparison with static ones.

In this paper, three sandwich beams with 0 wt%, 3 wt% and 5 wt% nano-silica in face-sheets and Polyurethane core were fabricated and static and dynamic delamination threshold forces were obtained by TPB tests. Furthermore, three sandwich panels with 0 wt%, 3 wt% and 5 wt% nano-silica in face-sheets were

fabricated and LVI tests in three energy levels of 4.70J, 15.70J and 24.53J were performed on them. A new criterion was introduced which states that if the maximum of contact force obtained by LVI test is greater than the corresponding dynamic delamination threshold force obtained by TPB test, delamination damage mode occurs in top face-sheet sandwich panel. In addition, the effect of nano-silica particles on delamination threshold forces, ILSS's, contact forces, contact duration, lateral deflection of contact point and energy absorption of top face-sheets and damage area caused by delamination has been investigated. In the last section the damage area caused by delamination was calculated theoretically and improved by using a correction factor obtained from experimental results using two different methods.

2. Experimental Results and Discussion

In this paper three sandwich beams and three sandwich panels with 0 wt%, 3 wt% and 5 wt% nano silica in face-sheets were fabricated and static TPB tests on sandwich beams and low velocity impact (LVI) tests on sandwich panels were performed. The procedure of face-sheets fabrication is as follows [15]: For dehumidification of nano-silica, it was dried in oven for 2 hours at 105°C and then mixed in pure epoxy at 0, 3 and 5 weight percent using a mechanical blender for 20 minutes. After that the mixture was sonicated for 20 minutes using an ultrasonic probe for perfect distribution of nano-silica in epoxy and the mixture degasification. Then the hardener was added to mixture by 1:10 weight ratio and final mixture and woven E-glass fabric were used to mold 22cm×22cm face-sheets for sandwich panels and 20cm×2.5cm face-sheets for sandwich beams using hand lay-up technique at 40:60 volume ratio. The dimensions of sandwich beams were chosen due to ASTM D7250 [16]. The molds were put in oven at 100°C for 5 hours for complete curing. The Polyurethane 180 (PU 180) foam was attached to face-sheets using pure epoxy. The mechanical properties of face-sheets and PU 180 foam are presented in reference [15] and Table 1, respectively. The sandwich beam specimens with 0 wt%, 3 wt% and 5 wt% of nano-silica in face-sheets are named as B1, B2 and B3 respectively illustrated in Table 2. Moreover, in Table 2 the sandwich panels with 0 wt%, 3 wt% and 5 wt% of nano-silica in face-sheets are named as S1, S2 and S3, respectively.

Table 1
Mechanical properties of Polyurethane foam core of sandwich panel.

Foam	Density (kg/m ³)	Thickness (mm)	Young's modulus (MPa)	Compressive yield stress (MPa)	Tensile yield stress (MPa)
PU180	180	20	156.86MPa	7.804	1.925

Table 2

Sandwich beams and panels specimens specifications.

Specimen	Face-sheets/Thickness(mm)	Core/Thickness(mm)	In-plane dimensions
B1	Epoxy-fiberglass/1mm	PU180/20mm	20cm×2.5cm
B2	Epoxy-fiberglass-3 wt% nanosilica/ 1mm	PU 180/20mm	20cm×2.5cm
B3	Epoxy-fiberglass-5 wt% nanosilica/1mm	PU 180/20mm	20cm×2.5cm
S1	Epoxy-fiberglass/1mm	PU180/20mm	22cm×22cm
S2	Epoxy-fiberglass-3 wt% nanosilica/1mm	PU 180/20mm	22cm×22cm
S3	Epoxy-fiberglass-5 wt% nanosilica/1mm	PU 180/20mm	22cm×22cm

2.1. Three-point Bending Tests

Three-point Bending (TPB) test is a classic standard test which results the flexural properties of sandwich beams. A schematic of this test is shown in Fig. 1 where a beam with the thickness of t rests on two roller supports with the radius r and the distance of S called Span. The middle of beam is facing a normal concentrated load P , exerted by a nose with the radius of R . In this test, by increasing the load P , the lateral deflection increases until the failure occurs. Force-deflection diagram of three sandwich panels with face-sheets made of fiberglass-epoxy and 0 wt% nanosilica (B1), 3 wt% nano-silica (B2) and 5 wt% nanosilica (B3) is shown in Fig. 2. The first drops shown by circles are considered as the static delamination threshold point as explained in previous works [17]. As seen, by increasing the nano-silica wt%, the static threshold delamination load ($F_{del-static}$) increases which may be due to the fact that by incorporation of nano-silica particles the interlaminar bondings in composite face-sheets are reinforced and the necessary load to initiate and propagate the crack increases. In fact, due to high area to volume ratio of nano-silica particles, the bondings per unit volume between two adjacent layer increases, which cause the threshold delamination force to be greater to initiate the crack in comparison with the absence of nano-silica particles. On the other hand after initiating a crack, the nano-silica particles can resist against crack propagation due to their great bonding sites per unit volume. The calculated stiffness of B1 and B2 samples are very close together and their difference is negligible. It may be due to insufficient nano-bonding contents. The test procedure of 3 wt% specimen is shown in Fig. 3 which delamination mode of damage can be detected. The experimental results show that by increasing the nano-silica wt% from 0 to 5, static threshold delamination force increases by 49%. After determining the static delamination threshold force, the Interlaminar Shear Strength (ILSS) can be calculated using the following equation [13]:

$$ILSS_{static} = \left(\frac{F_{del-static}^2 E}{6\pi^3 t^3 R} \right)^{1/3} \quad (1)$$

where $R = 5\text{mm}$ is the nose radius, $t = 1\text{mm}$ is the thickness of the composite face-sheet and E is the transverse elastic modulus. Threshold delamina-

tion force is proportional to $ILSS_{static}^{3/2}$ [13]. On the other hand the dynamic ILSS can be approximated 25% greater than static ILSS [3],

$$ILSS_{Dynamic} \cong 1.25 ILSS_{static} \quad (2)$$

So, the dynamic threshold delamination force is approximately $1.25^{3/2} \cong 1.4$ times the static threshold delamination force:

$$F_{del-Dynamic} \cong 1.4 F_{del-static} \quad (3)$$

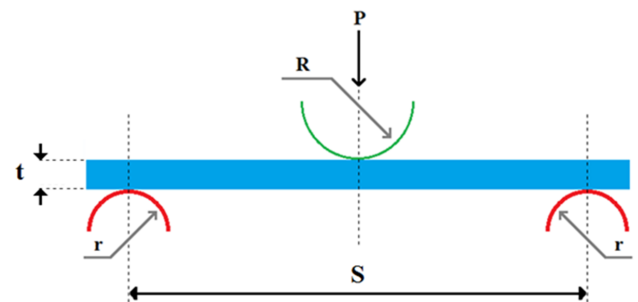


Fig. 1. Three point bending test specifications.

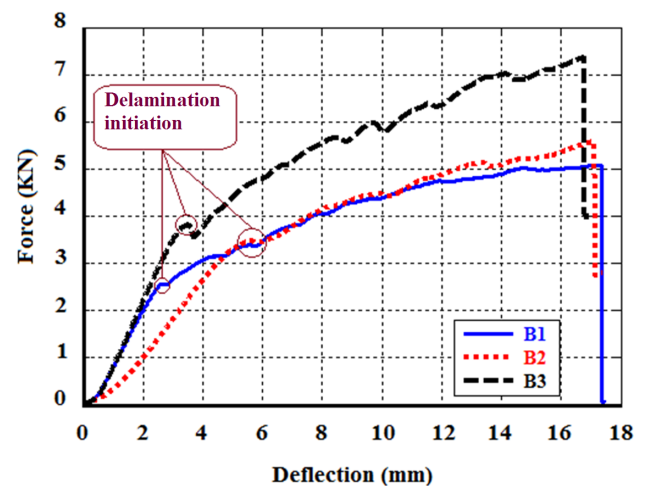


Fig. 2. Force-deflection diagram of TPB test of sandwich beams.

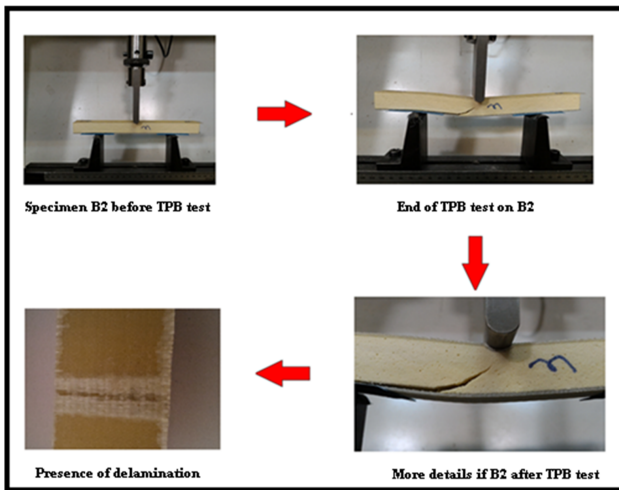


Fig. 3. Three point bending test procedure on B2.

The magnitudes of static and dynamic delamination threshold forces and ILSS's are presented in Table 3. As seen both static and dynamic ILSS's increase by increasing the nano-silica wt% which may be due to similar reason to increment of delamination threshold forces by increment of nano-silica wt% which was expressed above about threshold static delamination force. The results show that by increasing the nano-silica wt% from 0 to 5, the dynamic delamination threshold force and dynamic ILSS increase by 49% and 45.27%, respectively. The dynamic delamination threshold forces will be used as a criterion to predict whether delamination mode of damage occurs in LVI test or not. The reason of using this criterion is the independency of localized loadings (TPB and LVI) to planar geometry and boundary conditions [5-7].

2.2. Low Velocity Impact Tests

Nine different LVI tests with three replicates in three energy levels 4.70J, 15.70J and 24.53J were conducted on specimens S1, S2 and S3 using a drop hammer apparatus shown in Fig. 4. The hemispherical-tip impactor is made of stainless steel with the diameter of 13mm and the Young's modulus of 195GPa. Additionally, the opening of the clamped supports is 15cm×15cm. After performing the LVI tests, contact force history diagrams were obtained which are illustrated in Fig.

5a to 5c. The conditions and results of LVI tests including maximum contact forces and impact durations are illustrated in Table 5.

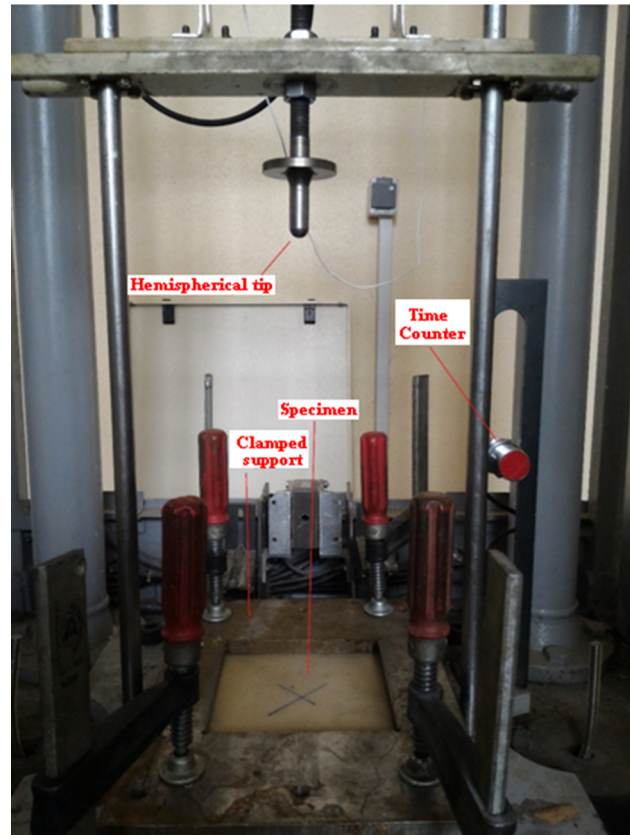


Fig. 4. Low velocity impact test apparatus.

As seen in Table 4 and Fig. 5, by increasing the nano-silica wt% from 0 to 5 wt% the maximum contact forces of sandwich panel increase by 42.23%, 39.64% and 42.25% for energy levels of 4.70J, 18.70J and 24.53J, respectively. Furthermore, by increasing the nano-silica content from 0 to 5 wt%, the impact duration decreases by 4.19%, 2.50% and 4.21% for energy levels of 4.70J, 18.70J and 24.53J, respectively. This phenomenon is due to increasing the rigidity and stiffness of face-sheets by increasing the nano-silica content from 0 to 5 wt% and subsequently faster returning of impactor or faster velocity changing, which is equivalent to higher acceleration and higher maximum contact force.

Table 3
Static and dynamic delamination threshold forces and ILSS's of sandwich beams.

Sample	Static delamination threshold force (KN)	Static ILSS (MPa)	Dynamic delamination threshold force (KN)	Predicted dynamic ILSS (MPa)
B1	2.553	266.882	3.574	333.603
B2	3.471	342.316	4.860	427.598
B3	3.804	387.698	5.326	484.623

Table 4

The conditions and results of LVI tests.

Test No.	Specimen	Mass of impactor (kg)	Height (m)	Impact velocity (m/s)	Energy (J)	Maximum contact force (KN)	Impact duration (ms)
1	S1	1.92	0.25	2.22	4.70	2.96	2.171
2	S2	1.92	0.25	2.22	4.70	3.38	2.106
3	S3	1.92	0.25	2.22	4.70	4.21	2.080
4	S1	4	0.40	2.80	15.70	3.779	4.127
5	S2	4	0.40	2.80	15.70	4.409	4.066
6	S3	4	0.40	2.80	15.70	5.277	4.024
7	S1	5	0.50	3.13	24.53	4.301	5.850
8	S2	5	0.50	3.13	24.53	4.912	5.675
9	S3	5	0.50	3.13	24.53	6.118	5.604

Table 5

Predicted dynamic delamination threshold force and delamination conditions for each test number.

Test No.	Dynamic delamination threshold force (KN)	Delamination occurred?	
		Criterion prediction	Visual test
1	3.191	No	No
2	4.34	No	No
3	4.755	No	No
4	3.191	Yes	Yes
5	4.34	Yes	Yes
6	4.755	Yes	Yes
7	3.191	Yes	Yes
8	4.34	Yes	Yes
9	4.755	Yes	Yes

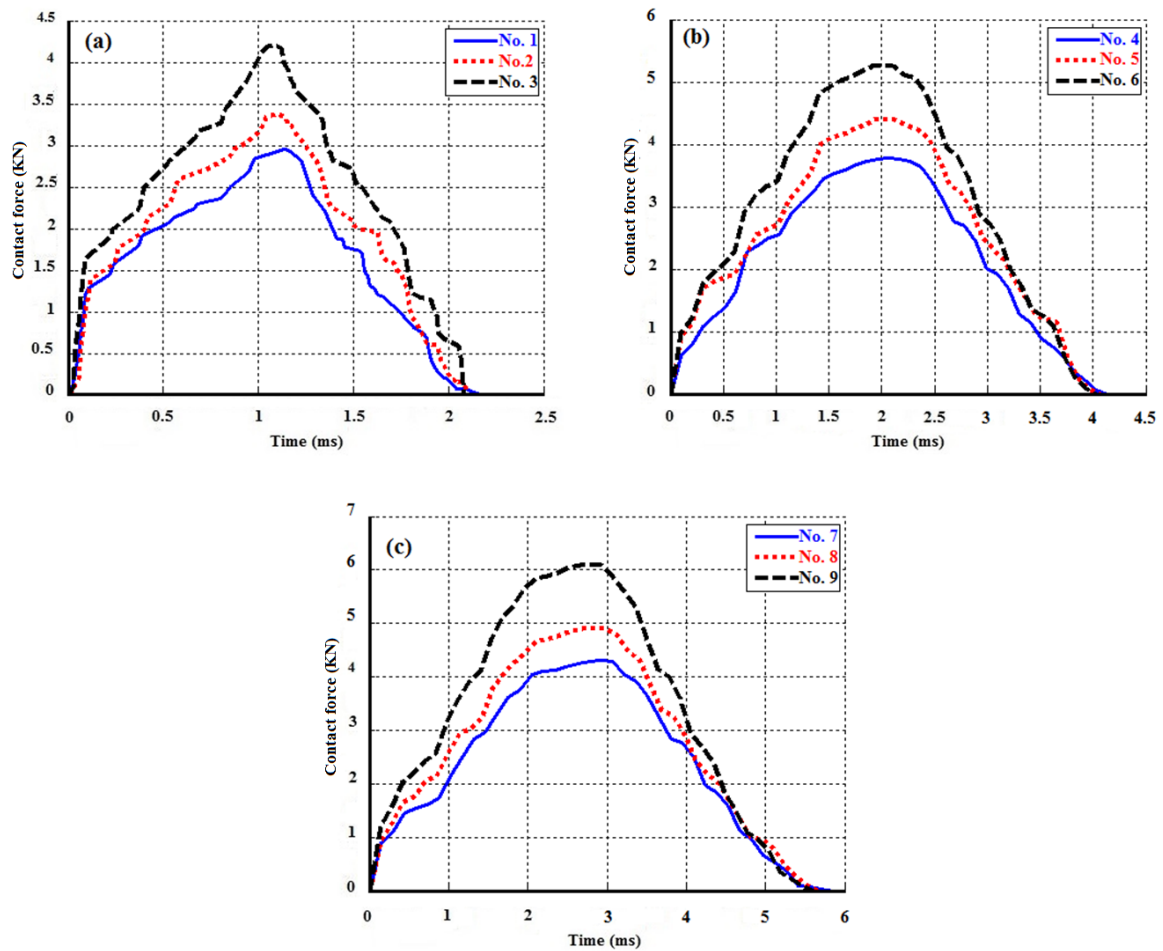


Fig. 5. Contact force history of sandwich panels at a) 4.70J, b) 15.70J, and c) 24.53J impact energy.

Also by increasing the impact energy level, impact duration and the maximum contact force increase. Impact duration change may be related to inertia effects and, increasing transferred energy results in maximum contact force increment.

In the next part, it should be checked whether the predicted dynamic threshold delamination forces determined by TPB test have a reasonable accuracy to predict the existence of delamination in LVI tests or not. In the experiments of this paper, the aim is not to predict the exact required force to initiate the delamination in LVI tests but it is desired to check whether due to predicted dynamic threshold delamination forces, delamination has occurred. Therefore, a criterion was introduced in a way that if the maximum contact force in LVI test is greater than predicted dynamic threshold force obtained from static TPB test, the delamination will occur.

The delamination mode of damage forms a peanut shape at the contact area [18]. For the test No. 1 to test No. 3 in Table 4 delamination did not occur during LVI tests. On the other hand, as illustrated in Table 5, the maximum contact forces corresponding to test No. 1 to No. 3 of LVI experiments are lower than their corresponding predicted dynamic delamination threshold force. In these tests only negligible indentation can be detected. As seen in Table 5, in the test No. 4 to No. 9, maximum contact forces are greater than predicted dynamic delamination threshold force. So, this criterion predicts the existence of delamination in these tests. Visual observations validate this criterion. In Fig. 6 the peanut shape of delamination mode of damage is seen for test No. 5, No. 7 and No. 8. Moreover, in Fig. 6 the dimensions of damaged area caused by

delamination can be calculated which will be used in next section. Therefore, the dynamic threshold delamination criterion, which was introduced in this paper, can greatly predict the existence of delamination mode of damage.

2.3. Lateral Deflection of Contact Point and Energy Absorption During Low Velocity Impact

In this section the lateral deflection of contact point and absorbed energy of top face-sheet in LVI tests are calculated. The deflection of top face-sheet history at the contact point in LVI tests are drawn as [19],

$$\delta(t) = \delta_0 + \nu_0 t + \frac{gt^2}{2} - \int_0^t \int_0^t \frac{F_C(t)}{m} dt dt \quad (4)$$

where ν_0 , δ_0 , m , $\delta(t)$ and $F_C(t)$ are initial velocity of impactor, initial lateral displacement of impactor, mass of impactor, lateral deflection of contact point and contact force, respectively.

The lateral deflection of the contact point history at different energy levels is drawn in Fig. 7 using Eq. (4). Additionally, the maximum deflection of contact point for each test is illustrated in Table 6. As seen, by increasing the nano-silica content from 0 to 5 wt%, the maximum deflection of contact point decreases by 15.24%, 16.30% and 16.31% for energy levels of 4.70J, 18.70J and 24.53J, respectively which may be due to increment of rigidity and stiffness of face-sheet. Furthermore, by increasing the energy level, the maximum deflection of top face-sheet increases which is due to inertia effects.

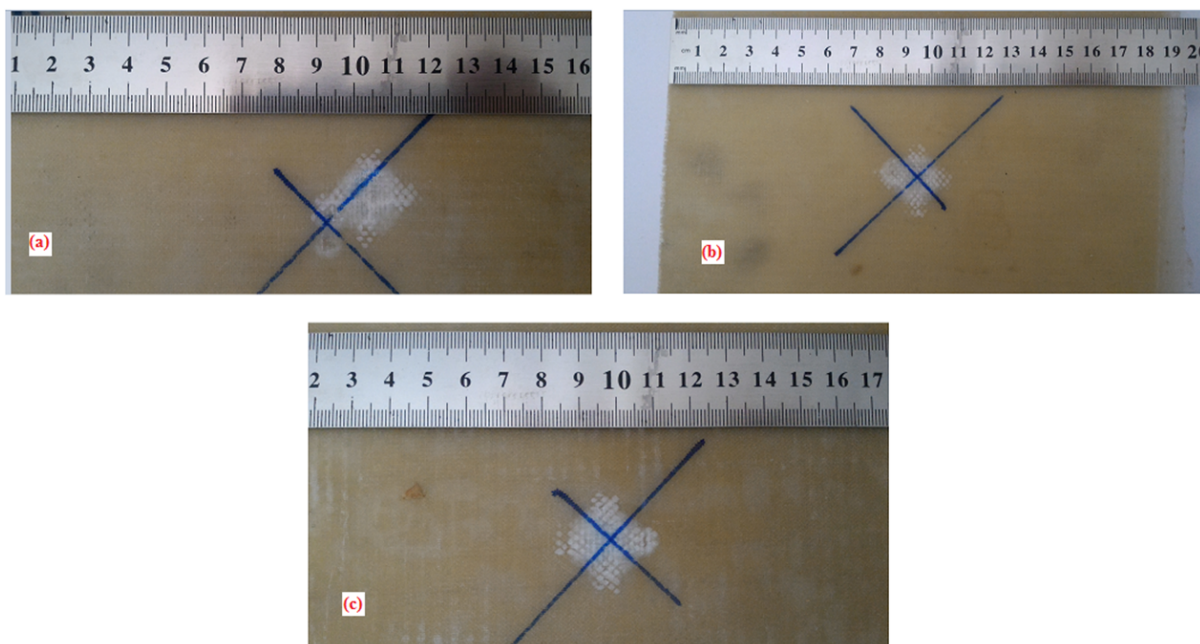


Fig. 6. Delamination in the a) Test No. 5, b) Test No. 7, and c) Test No. 8.

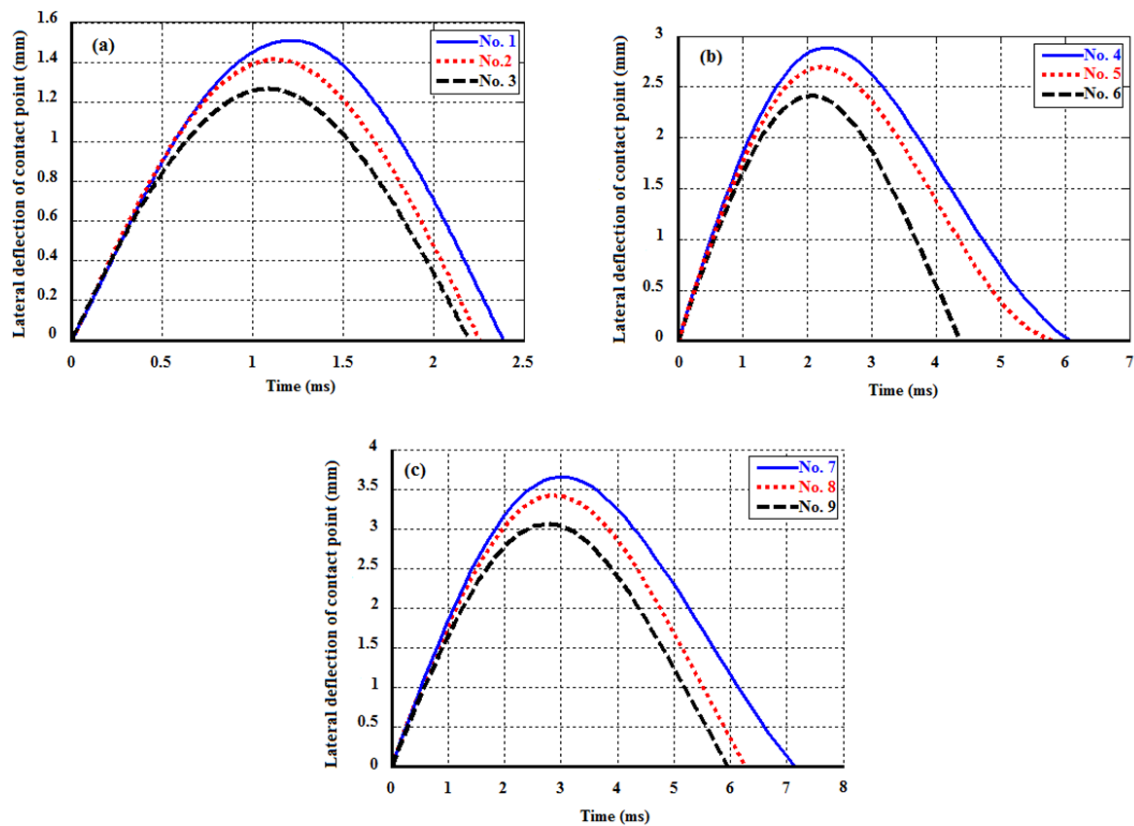


Fig. 7. Lateral deflection of contact point history of sandwich panel at a) 4.70J, b) 15.70J, and c) 24.53J impact energy.

By obtaining deflection of contact point, the contact force vs. deflection of contact point for each LVI test was drawn as shown in Fig. 8. By integration of contact force with respect to deflection of contact point, the absorbed energy of top face-sheet can be calculated. The values of these integrations are illustrated in Table 6. Also the portion of face-sheet in energy absorption is presented in Table 6.

As seen for each level of energy, by increasing the nano-silica content from 0 to 5 wt%, the portion of absorbed energy by top face-sheet increases. By increasing nano-silica contents, the bonding among epoxy,

fiberglass and nano-silica increases which causes improving the absorbed energy by face-sheets. In fact, the nano-silica may establish strong bondings among other contents in face-sheets which results in better energy absorption. By considering LVI tests on similar specimens (in terms of nano-silica wt%), e.g. 1, 4 and 7 which include LVI test on specimen S1 at different energy levels, it was seen that in tests including the delamination mode of damage, the portion of absorbed energy by face-sheet increases which may be due to part of energy required to initiate and propagate the delamination.

Table 6

The absorbed energy of top face-sheet in 15.70J and 24.53J impact energy.

Test No.	Experimental			Maximum deflection of contact point at top face-sheet (mm)
	Absorbed energy by top face-sheet (J)	Total energy (J)	Portion of absorbed energy (%)	
1	0.636	4.70	13.53%	1.699
2	1.074	4.70	22.85%	1.551
3	1.164	4.70	24.76%	1.44
4	3.48	15.70	22.17%	2.884
5	4.54	15.70	28.91%	2.695
6	5.22	15.70	33.25%	2.414
7	5.28	24.53	21.52%	3.654
8	6.95	24.53	28.33%	3.415
9	7.75	24.53	31.59%	3.058

2.4. Impact Damage Area Caused by Delamination

In this section the experimental damage area due to delamination is compared with Xiao et al. [18] model and new modified formulation for determination of damage area in sandwich panel is presented. Xiao et al. [18] showed that the peanut damaged area in rectangular composite plate can be approximated by a circular area as follows and verified this equation can be verified by LVI tests on IMS/X850 composite plate at different energy levels:

$$S_C = \pi r_c^2 = \frac{9}{16\pi} \left(\frac{F_{max}}{t \cdot \tau_{allowable}} \right)^2 \quad (5)$$

where F_{max} , t and $\tau_{allowable}$ are the maximum contact force, thickness of face-sheet and allowable interlaminar shear stress, respectively. Davies and Zhang [20] stated that $\tau_{allowable}$ could be equal to static ILSS; but experimental results did not verify this selection and consequently the half of the static ILSS was considered for the allowable interlaminar shear stress. In this paper the $\tau_{allowable}$ is assumed as a fraction of static ILSS, so:

$$\tau_{allowable} = k \cdot ILSS_{static} \quad (6)$$

where k is the correction factor and must be determined for sandwich panels. By substituting Eq. 6 in Eq. 7,

$$S_C = \pi r_C^2 = \frac{9}{16\pi} \left(\frac{F_{max}}{t \cdot k \cdot ILSS_{static}} \right)^2 \quad (7)$$

To calculate k , the experimental damage area is set to be equal to Eq. 7 for each test containing delamination mode of damage (No. 4 to No. 9 in Table 4), k is calculated which the results are illustrated in Table 7. One of the ways to choose the correction factor is the averaging of obtained k 's in Table 7. By performing the averaging, the correction factor is obtained as $k=0.318$. By substituting this value in Eq. 7,

$$S_C = \pi r_C^2 = \frac{9}{16\pi} \left(\frac{F_{max}}{0.318t \cdot ILSS_{static}} \right)^2 \quad (8)$$

Table 7

Experimental damage area and correction factor k .

Test No.	Experimental damage area (cm ²)	k
4	3.819	0.307
5	3.397	0.296
6	3.282	0.318
7	4.233	0.331
8	3.88	0.308
9	3.667	0.349

By calculating the theoretical damage area based on Eq. (8) and comparison with experimental damage area (illustrated in Table 7), the error of theoretical model is obtained which is illustrated in Table 8. As seen, the minimum, maximum and average error are 0.12%, 20.18% and 9.27%, respectively.

Another way to calculate the correction factor k is to assume that k is a function of nano-silica weight percentage (w). In this manner the similar experiments in terms of specimen used, were considered and the values of k were calculated for each specimen in similar experiments illustrated in Table 9. By a simple curve fitting, the following equation can be written:

$$k(w) = 43.333w^2 - 1.866w + 0.319 \quad (9)$$

Therefore, the Eq. (5) and Eq. (6) is rewritten as:

$$\tau_{allowable} = K(w) ILSS_{static} \quad (10)$$

$$S_C = \pi r_C^2 = \frac{9}{16\pi} \left(\frac{F_{max}}{k(w) \cdot t \cdot ILSS_{static}} \right)^2 \quad (11)$$

It should be mentioned that F_{max} and $ILSS_{static}$ are also functions of nano-silica weight percentage. In Table 10, the computed damage areas by this method are compared with experimental results. The maximum, minimum and average error for prediction of damage area by Eq. (10) is 9.39%, 4.13% and 7.05% in LVI tests.

Two methods for determining the correction factor were used. The first method states that $k = 0.318$ and the second method states that k is a function of nano silica weight percentage in face-sheets. As seen in Table 8 and Table 10 and by comprising the maximum, minimum and average errors of two methods, one can say that the second method is more accurate than the first model.

Table 8

Error of theoretical model (Eq. 8) in prediction of damage area.

Test No.	Theoretical damage area (cm ²) (Eq. (8))	Experimental damage area (cm ²) (Table 7)	Error %
4	3.548	3.819	7.10%
5	2.935	3.397	13.60%
6	3.278	3.282	0.12%
7	4.595	4.233	8.55%
8	3.644	3.88	6.08%
9	4.407	3.667	20.18%

Additionally, as seen in Table 7, by increasing the nano-silica from 0 to 5 wt%, the delamination damage area under LVI tests decreases by approximately 13.61% which may be due to increasing the rigidity and resistance of face-sheets against delamination propagation in the presence of nano silica particles.

Table 9Correction factor k for the experiments with the same specimens.

Test No.	Specimen	Nano-silica wt%	k
4, 7	S1	0	0.319
5, 8	S2	3	0.302
6, 9	S3	5	0.334

Table 10

Comparison of damage area computed from Eq. (11) with experimental results.

Test No.	Damage area (cm ²) computed from Eq. (11)	Experimental damage area (cm ²)	Error %
4	3.528	3.819	7.62%
5	3.2568	3.397	4.13%
6	2.9738	3.282	9.39%
7	4.570	4.233	7.96%
8	4.043	3.88	4.20%
9	3.997	3.667	9.00%

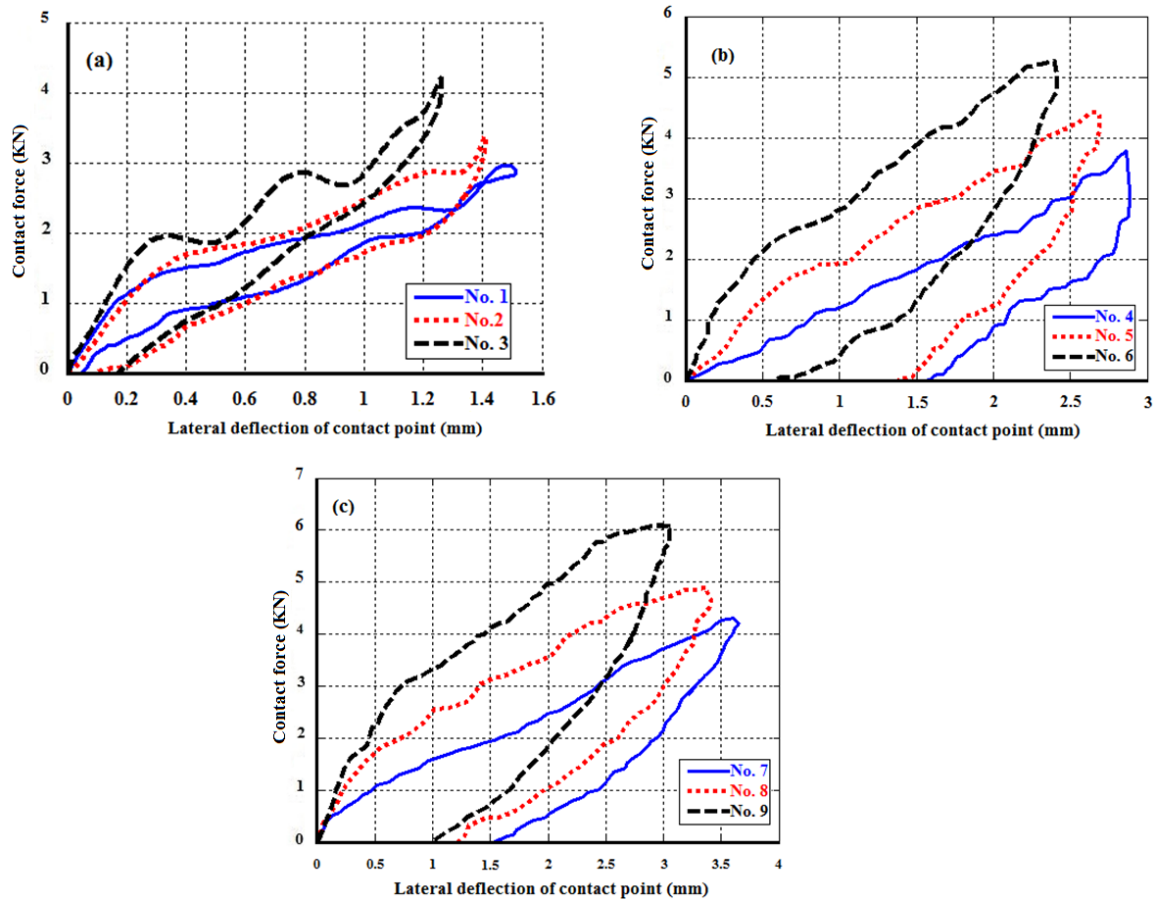


Fig. 8. Contact force vs. lateral deflection of top face-sheet of sandwich panel at a) 4.70J, b) 15.70J, and c) 24.53J impact energy.

3. Conclusions

In this paper the results of TPB and LVI tests on Polyurethane cored sandwich beams and sandwich panels with hybrid nanocomposites face-sheets made of epoxy/woven fiberglass/ nano-silica were presented and impact damage response of sandwich panel was investigated. The values of static threshold delamination force and static interlaminar shear strength for

sandwich panel were determined. Furthermore, the dynamic threshold delamination force and dynamic interlaminar shear strength were set approximately 1.4 and 1.25 times the static values, respectively. The dynamic threshold delamination force determined by TPB test had a reasonable accuracy to predict the existence of delamination in LVI test.

According to experimental results, the following conclusions can be drawn:

- The experimental results from TPB test of sandwich beam with epoxy/woven-fiberglass/nano-silica nanocomposites face-sheets and PU foam core show that by increasing the nano-silica wt% from 0 to 5, static threshold delamination force and static ILSS increase by 49% and 45.27%, respectively. These results are the same for dynamic values.
- From the experimental results of LVI test, it can be concluded that if the maximum contact force in LVI test is greater than the dynamic threshold delamination force from TPB test, delamination occurs.
- By increasing the nano-silica wt% from 0 to 5 in face-sheets of sandwich panel, in LVI test the maximum contact force and portion of absorbed energy by top face-sheet increase by approximately 41.35% and 59.92%, respectively. Also impact duration and the maximum deflection of top face-sheet at contact point decreases by approximately 3.63% and 15.95%, respectively.
- From the experimental observation by increasing the nano-silica from 0 to 5 wt%, the delamination damage area under LVI decreases by approximately 13.61%.
- The delamination damage area was computed by two different methods. The first method assumes that the correction factor in determining the allowable shear stress which is used in calculation of damage area is constant. The second method assumes that the mentioned correction factor is a function of nano silica wt%. The results show that the second method has better consistency with experimental observation in LVI test on sandwich panel with epoxy/woven fiberglass/ nano silica and Polyurethane core than the first method.

References

- [1] A. Azzam, W. Li, An experimental investigation on the three-point bending behavior of composite laminate, IOP Conference Series: Materials Science and Engineering, IOP Publishing, Ningbo, China, 62 (2014) 012016.
- [2] A. Farrokhhabadi, S.A. Taghizadeh, H. Madadi, H. Norouzi, A. Ataei, Experimental and numerical analysis of novel multi-layer sandwich panels under three point bending load, *Compos. Struct.*, 250 (2020) 112631.
- [3] Ł. Pyrzowski, B. Sobczyk, Local and global response of sandwich beams made of GFRP facings and PET foam core in three point bending test, *Compos. Struct.*, 241 (2020) 112122.
- [4] T.S. Lim, C.S. Lee, D.G. Lee, Failure modes of foam core sandwich beams under static and impact loads, *J. Compos. Mater.*, 38(18) (2004) 1639-1662.
- [5] F.J. Yang, W.J. Cantwell, Impact damage initiation in composite materials, *Compos. Sci. Technol.*, 70(2) (2010) 336-342.
- [6] G. Minak, D. Ghelli, Influence of diameter and boundary conditions on low velocity impact response of CFRP circular laminated plates, *Compos. B. Eng.*, 39(6) (2008) 962-972.
- [7] S. Zhu, G.B. Chai, Damage and failure mode maps of composite sandwich panel subjected to quasi-static indentation and low velocity impact, *Compos. Struct.*, 101 (2013) 204-214.
- [8] F. Zhu, G. Lu, D. Ruan, Z. Wang, Plastic deformation, failure and energy absorption of sandwich structures with metallic cellular cores, *Int. J. Prot. Struct.*, 1(4) (2010) 507-541.
- [9] X. Fan, I. Verpoest, D. Vandepitte, Finite element analysis of out-of-plane compressive properties of thermoplastic honeycomb, *J. Sandwich Struct. Mater.*, (2005) 875-884.
- [10] S.R. Swanson, Limits of quasi-static solutions in impact of composite structures, *Compos. Eng.*, 2(4) (1992) 261-267.
- [11] B.C. Ray, Effects of crosshead velocity and sub-zero temperature on mechanical behaviour of hygrothermally conditioned glass fibre reinforced epoxy composites, *Mater. Sci. Eng. A*, 379(1-2) (2004) 39-44.
- [12] S.R. Hallett, C. Ruiz, J. Harding, The effect of strain rate on the interlaminar shear strength of a carbon/epoxy cross-ply laminate: comparison between experiment and numerical prediction, *Compos. Sci. Technol.*, 59(5) (1999) 749-758.
- [13] L.S. Sutherland, C.G. Soares, Contact indentation of marine composites, *Compos. Struct.*, 70(3) (2005) 287-294.
- [14] P.M. Schubel, J.J. Luo, I.M. Daniel, Low velocity impact behavior of composite sandwich panels, *Composites, Part A*, 36(10) (2005) 1389-1396.
- [15] S. Feli, M.M Jalilian, Experimental and optimization of mechanical properties of epoxy/nanosilica and hybrid epoxy/fiberglass/nanosilica composites, *J. Compos. Mater.*, 50(28) (2016) 3891-3903.

- [16] ASTM D7250/D7250M-20, Standard Practice for Determining Sandwich Beam Flexural and Shear Stiffness, ASTM International, West Conshohocken, PA, (2016).
- [17] G.B. Murri, E.G. Guynn, Analysis of delamination growth from matrix cracks in laminates subjected to bending loads, In Composite Materials: Testing and Design (Eighth Conference), ed. J. Whitcomb, West Conshohocken, PA: ASTM International, (1988) 322-339.
- [18] S. Xiao, P. Chen, Q. Ye, Prediction of damage area in laminated composite plates subjected to low velocity impact, *Compos. Sci. Technol.*, 98 (2014) 51-56.
- [19] E.M. Soliman, M.P. Sheyka, M.R. Taha, Low-velocity impact of thin woven carbon fabric composites incorporating multi-walled carbon nanotubes, *Int. J. Impact Eng.*, 47 (2012) 39-47.
- [20] G.A.O. Davies, X. Zhang, Impact damage prediction in carbon composite structures, *Int. J. Impact Eng.*, 16(1) (1995) 149-170.